IOP Conf. Series: Materials Science and Engineering **145** (2016) 042034 doi:10.1088/1757-899X/145/4/042034

A robust algorithm for the contact of viscoelastic materials

S Spinu[1, 2] **and D Cerlinca**[1, 2]
[1]Department of Mechanics and Technologies, Stefan cel Mare University of Suceava, 13th University Street, 720229, Romania
[2]Integrated Center for Research, Development and Innovation in Advanced Materials, Nanotechnologies, and Distributed Systems for Fabrication and Control (MANSiD), Stefan cel Mare University, Suceava, Romania

E-mail: sergiu.spinu@fim.usv.ro

Abstract. Existing solutions for the contact problem involving viscoelastic materials often require numerical differentiation and integration, as well as resolution of transcendental equations, which can raise convergence issues. The algorithm advanced in this paper can tackle the contact behaviour of the viscoelastic materials without any convergence problems, for arbitrary contact geometry, arbitrary loading programs and complex constitutive models of linear viscoelasticity. An updated algorithm for the elastic frictionless contact, coupled with a semi-analytical method for the computation of viscoelastic displacement, is employed to solve the viscoelastic contact problem at a series of small time increments. The number of equations in the linear system resulting from the geometrical condition of deformation is set by the number of cells in the contact area, which is a priori unknown. A trial-and-error approach is implemented, resulting in a series of linear systems which are solved on evolving contact areas, until static equilibrium equations and complementarity conditions are fully satisfied for every cell in the computational domain. At any iteration, cells with negative pressure are excluded from the contact area, while cells with negative gap (i.e. cells where the contacting bodies are predicted to overlap) are reincluded. The solution is found when pressure is stabilized in relation to the imposed normal load. This robust algorithm is expected to solve a large variety of contact problems involving viscoelastic materials.

1. Introduction

The classic approach in solving the viscoelastic contact problem is based on the solution of the associated elastic problem, solved in the frame of linear elasticity by Sneaddon [1]. This method relies on the removal of time dimension via Laplace transform, which reduces the viscoelastic problem to a formally identical elastic problem whose solution is easier to achieve. Consequently, if the boundary conditions are time-independent, a viscoelastic solution in the frequency domain is identical in form to that of the associated elastic problem. This technique of deriving viscoelastic solutions in the frequency domain from their elastic counterparts is also referred to as the correspondence principle. The desired viscoelastic solutions in the time/space domain is subsequently obtained by applying inverse Laplace transform to its spectral counterpart. Additional complications arise as most contact problems exhibit transient boundary conditions, which cannot be directly treated by means of Laplace transform. Consequently, the method of functional equations [2-4] applied to contact mechanics leads to solutions subjected to limitations. Lee and Radok [2] solved the Hertz contact problem for linear viscoelastic materials under the assumption that the contact area increases monotonically with time.

The case when the contact radius possess a single maximum was subsequently solved by Hunter [3]. Yang [4] extended the results to general linear materials and arbitrary quadratic contact geometry. A solution of increased generality, allowing for contact radii described by arbitrary functions of time and multiply connected contact regions, was later achieved by Ting [5,6], but in an implicit form. The contact problem between an axisymmetric indenter and a viscoelastic half-space was recently revisited by Greenwood [7]. The mathematical complexity of these partially analytical solutions impedes wide range application, especially when the contact undergoes complicated loading histories. The classic approach involves numerical differentiation and integration, as well as numerical resolution of transcendental equations, for which a careful selection of numerical algorithms is required to avoid convergence issues. On the other hand, the iterative scheme used in this paper employs quadratic optimization, whose convergence is guaranteed.

The numerical treatment of the viscoelastic contact problem is supported by recent developments in computational contact mechanics, based on the so-called semi-analytical methods (SAM) derived from the boundary element method (BEM). According to this review [8], the computational efficiency of SAM greatly exceeds that of the finite element method (FEM), to the point where a three-dimensional SAM contact simulation can be conducted with the same computational effort as a two-dimensional finite element analysis. Recent application of SAM in the field of viscoelastic contact mechanics were reported by these authors [9-11]. The method employed in this paper features an updated version of the contact solver [12] based on the conjugate gradient method (CGM). The latter solver was previously used in simulation of path-dependent processes like the elastic-plastic contact [13] or the slip-stick elastic contact [14], by imposing incremental load application to replicate the process path. This paper extends the contact model generality by recomputing the mechanical response of the contacting material for each new time increment, as required by the viscoelastic constitutive law.

The proposed method for viscoelastic contact simulation consists in integration of the aforementioned contact solver with a recently developed [15] semi-analytical formula for computation of viscoelastic displacement induced by a known, but otherwise arbitrary distribution of normal surface tractions (i.e. pressure). The computational efficiency of the newly advanced algorithm is increased by using a well-established method [16] for rapid calculation of convolution products, allowing for fine spatial and temporal discretizations capable of simulating rough contact problems. This robust algorithm is expected to tackle a large variety of contact scenarios involving viscoelastic materials.

2. Contact model

The principles of contact problem discretization are detailed elsewhere [15]. It should be noted that the model features both spatial and temporal discretizations to achieve accurate simulation of the viscoelastic contact process.

The spatial discretization is needed as the contact area and the established pressure distribution are a priori unknown, and, moreover, keep changing during the contact process, as the mechanical response of the viscoelastic material vary with time as well. As contact area is computed in an iterative manner, integration over repeatedly changing contact area occurs during algorithm execution, which can only be achieved in a numerical manner. In a Cartezian coordinate system with the $\vec{x}_1$ and $\vec{x}_2$ axes laying in the common plane of contact, the computational domain P is chosen in the common plane of contact as a rectangular and uniformly spaced grid with $N_1 \times N_2$ elementary cells. Over each elementary cell, all problem parameters are assumed constant, thus yielding piecewise constant distributions. The sides of the elementary cell in the two directions are denoted by Δ_1 and Δ_2, with $\Delta = \Delta_1 \Delta_2$. A convenient notation is introduced, employing a set of integers $i = 1 \ldots N_1$, $j = 1 \ldots N_2$, for indexing all the grid cells. This notation assumes that a representative controlling point is chosen for every elementary cell (usually the center of the cell). Any continuous parameter is substituted by a set of discrete values computed in the control points, thus generating a discrete counterpart for each continuous distribution.

The temporal discretization is needed as computation of surface viscoelastic displacement relies on information regarding the pressure distribution in the past period of time. Consequently, the loading period needs to be discretized in small time intervals, sufficiently short so that contact pressure and viscoelastic mechanical properties may be assumed constant during each time step. A uniform temporal mesh of step Δ_t, with N_t time steps, is thus imposed, adding a third argument to problem parameters, e.g. $p(i,j,k)$ is the discrete counterpart of the continuous pressure $p(x_1', x_2', t')$, with $x_1' = i\Delta_1$, $x_2' = j\Delta_2$, $t' = k\Delta_t$, and denotes the elementary pressure in the cell (i,j) of the spatial mesh, achieved during the contact process after k time steps in the simulation window. It is required that at $t = 0$ (i.e. the beginning of the simulation window), the viscoelastic body was undisturbed.

With these notations, the model for the viscoelastic frictionless contact problem under normal loading consists in the following equations and inequalities:

1. The static force equilibrium, equation (1):

$$W(k) = \Delta \sum_{(i,j)\in A(k)} p(i,j,k), \quad k = 1 \ldots N_t . \tag{1}$$

2. The geometrical condition of deformation, equation (2):

$$h(i,j,k) = hi(i,j) + u(i,j,k) - \omega(k), \quad (i,j) \in P, k = 1 \ldots N_t . \tag{2}$$

3. The contact complementarity conditions, equation (3), (4):

$$p(i,j,k) > 0 \quad \text{and} \quad h(i,j,k) = 0, \quad (i,j) \in P, k = 1 \ldots N_t ; \tag{3}$$

$$p(i,j,k) = 0 \quad \text{and} \quad h(i,j,k) > 0, \quad (i,j) \in P - A, k = 1 \ldots N_t . \tag{4}$$

4. The viscoelastic contact displacement, equation (5):

$$u(i,j,k) = \sum_{n=2}^{N_t} \sum_{\ell=1}^{N_1} \sum_{m=1}^{N_2} K(i-\ell, j-m, k-n)\big(p(\ell,m,n) - p(\ell,m,n-1)\big), \ (i,j) \in P, k = 2 \ldots N_t . \tag{5}$$

Here, W denotes the applied normal force, A the digitized contact area (i.e. a set of cells best fitting the shape of the apparent contact area), hi the initial (i.e. at time $t = 0$) composite contact geometry (or the gap between the undeformed surfaces), h the gap between deformed surfaces, u the relative displacement in the direction normal to the common plane of contact, ω the rigid-body approach, and K the viscoelastic influence coefficient, as described in [15]. The influence coefficient $K(i-\ell, j-m, k-n)$ expresses the displacement induced in the (i,j) patch of the spatial mesh at time $k\Delta_t$, by a uniform pressure $(\Delta_1\Delta_2)^{-1}$ [Pa] which acted in the patch (ℓ,m) at time $n\Delta_t$. Equation (5) shows that, in order to compute the viscoelastic displacement at time $t = k\Delta_t$, all pressure distributions in the previous $(k-1)$ steps are required. To achieve the contact simulation, a solution for the instantaneous (i.e. with k fixed) contact state consisting in equations (1) - (4), is firstly derived, based on the assumption that the history of the pressure distribution is known, but otherwise arbitrary.

3. Solution of the instantaneous contact state

In a first step, the contact problem is solved for the current time moment, under the assumption that the contact history is known, i.e. k is fixed (but otherwise arbitrary), and all historical pressures $p(i,j,1) \ldots p(i,j,k-1), (i,j) \in P$ are known. The goal is to find the current pressure distribution $p(i,j,k), (i,j) \in P$. To this end, both pressure and contact area are iterated simultaneously. During this iteration, the size of the linear system arising from equation (2), which is directly linked to the number of cells in the contact area, varies. At any iteration, cells with negative pressure are excluded from the contact area, while cells with negative gap (i.e. cells where the contacting bodies are

predicted to overlap) are reincluded. The solution is found when pressure is stabilized in relation to the imposed normal load. This iterative approach is classical in the contact mechanics of elastic and elastic-plastic bodies, but its application to viscoelastic materials is novel. The main algorithm steps are detailed below.

1. Initialize algorithm auxiliary variables, equation (6):

$$\theta = 0;\ R_{old} = 1;\ d(i,j) = 0,\ p_{old}(i,j,k) = 0, (i,j) \in P. \tag{6}$$

2. Adopt the initial guess for contact pressure. This yields from the static force equilibrium, by considering that all cells in the computational domain are in contact at the first iteration, i.e. $A = P$.

3. Compute the relative displacement field. To this end, the matrix of influence coefficients K is convoluted with the pressure history $p(i,j,1)\ldots p(i,j,k), (i,j) \in P$. It should be remembered that the historical pressures are assumed known, and the current pressure $p(i,j,k), (i,j) \in P$ was derived in step 2. Consequently, the viscoelastic displacement can be computed according to equation (5).

4. Compute the rigid-body approach. Considering equations (2) and (3) for every cell in the contact area, $\omega(k)$ results as, equation (7):

$$\omega(k) = \left(\sum_{(i,j)\in A(k)} 1 \right)^{-1} \sum_{(i,j)\in A(k)} \left[u(i,j,k) + hi(i,j,k) \right]. \tag{7}$$

This step is required to linearize equation (2), thus leading to a linear systems having the nodal pressures as unknowns. The latter system can be solved efficiently using the CGM.

5. Start the CGM loop by computing the residual and its square Euclidean norm, equation (8):

$$r(i,j,k) = hi(i,j,k) + u(i,j,k) - \omega(k), (i,j) \in P;\ R = \sum_{(i,j)\in A(k)} \left(r(i,j,k) \right)^2. \tag{8}$$

6. Compute the descend direction d in the CGM, equation (9):

$$d(i,j,k) \leftarrow \begin{cases} r(i,j,k) - d(i,j,k)\theta R / R_{old}, & (i,j) \in A(k); \\ 0, & (i,j) \in P - A(k). \end{cases} \tag{9}$$

7. Memorize the norm of the residual for subsequent computation of descent direction: $R_{old} = R$.

8. Assess the length of the step α to be made in the descend direction computed in step 6, equation (10) and (11):

$$\alpha = \left(\sum_{(i,j)\in A(k)} c(i,j,k) d(i,j,k) \right)^{-1} \sum_{(i,j)\in A(k)} r(i,j,k) d(i,j,k), \text{ where} \tag{10}$$

$$c(i,j,k) = \sum_{\ell=1}^{N_1} \sum_{m=1}^{N_2} K(i-\ell, j-m, k)\, d(\ell, m, k),\ (i,j) \in P. \tag{11}$$

9. Memorize the current contact tractions in a new variable for subsequent error computation: $p_{old}(i,j,k) = p(i,j,k), (i,j) \in P$.

10. Update the system solution. The CGM loop is concluded by making a step of length α along the d descent direction, equation (12):

$$p(i,j,k) \leftarrow p(i,j,k) - \alpha d(i,j,k), (i,j) \in A(k). \tag{12}$$

The CGM loop constraints the nodal pressures to satisfy the geometric condition of deformation in equation (2), but does not assures that the complementarity conditions or the static force equilibrium

are satisfied. The complementarity conditions are enforced in the next steps, by reassessing the contact or non-contact status of every cell in the computational domain.

11. Impose the complementarity conditions in equations (3) and (4). As the contact solver allows only compressive tractions, cells with negative pressure are removed from the contact area, and the corresponding nodal pressures are set to zero,

$$\begin{cases} A \leftarrow A - \{(i,j)\}, & (i,j) \in \{(i,j) : p(i,j,k) < 0\}; \\ p(i,j,k) = 0, & (i,j) \in \{(i,j) : p(i,j,k) < 0\}. \end{cases} \tag{13}$$

12. On the other hand, as bodies are considered impenetrable in the frame of Linear Theory of Elasticity, cells (i,j) having vanishing pressure $p(i,j,k) = 0$ but negative gap $h(i,j,k) < 0$, reenter the contact area. The corresponding pressures are updated with a positive amount, as discussed in [12]:

$$\begin{cases} A \leftarrow A \cup \{(i,j)\}, & (i,j) \in \{(i,j) : p(i,j,k) = 0 \text{ and } h(i,j,k) < 0\}; \\ p(i,j,k) \leftarrow p(i,j,k) - \alpha h(i,j,k), & (i,j) \in \{(i,j) : p(i,j,k) = 0 \text{ and } h(i,j,k) < 0\}. \end{cases} \tag{14}$$

13. Update the auxiliary variable θ. When the contact or non-contact status of specific cells changes in steps 11 or 12, the number of equations in the linear system resulted from equation (2) also changes. As the corresponding nodal pressures have no precedent in the residual minimization process of the CGM, a new search for the optimal path must be conducted. This is accomplished by resetting the conjugate directions d by means of the auxiliary variable θ, which is set to zero if any cell is removed from or reenters the contact area, or to unity otherwise.

14. Impose the static force equilibrium. The nodal pressure distribution is adjusted in relation to the imposed normal load, to satisfy equation (1):

$$p(i,j,k) \leftarrow p(i,j,k) W(k) \left(\sum_{(i,j) \in A(k)} p(i,j,k) \right)^{-1}. \tag{15}$$

15. Verify solution convergence to an imposed precision ε:

$$W(k)^{-1} \sum_{(i,j) \in A(k)} \left| p(i,j,k) - p_{old}(i,j,k) \right| \le \varepsilon. \tag{16}$$

If the nodal pressures vary insignificantly (with respect to the imposed normal load) from one iteration to the next, the algorithm stops. If else, a new iteration is executed starting from step 3.

The complementarity conditions in equations (3) and (4) show that only compressive normal traction (i.e. pressure) is allowed on the contact area, meaning adhesion is not accounted for. While adhesion can have a non-trivial contribution in case of rubber-like materials, the development of a contact solver incorporating adhesion is beyond the point of this paper. It should be noted that adhesion was not considered either in the classic literature [2-7] of viscoelastic contact.

The solution of the instantaneous contact state with vanishing load (i.e. after contact opening) can be obtained directly by setting pressure to zero, i.e. $p(i,j,k) = 0, (i,j) \in P$.

Regarding the algorithm computational efficiency, the most computationally intensive process is the convolution calculation in equations (5) and (11). When direct multi-summation is applied, the computational complexity of the convolution calculation is of order $O(N_1^2 N_2^2)$. The algorithmic efficiency can be increased dramatically by implementing the DCFFT technique [16], leading to an improved order of operations of $O(N_1 N_2 \log(N_1 N_2))$.

4. Simulation of the viscoelastic contact process

It was shown in the previous section that the solution of any instantaneous contact state can be derived based on the knowledge of all previous states. Capitalizing on this result, the simulation of the viscoelastic contact process can be achieved by solving a series of sequential contact states related to a temporal discretization, fine enough so that the memory effect specific to viscoelastic materials is accurately captured. The main algorithm steps are detailed below.

1. Acquire the input of the viscoelastic contact problem: the loading history $W(t), t \in [0,t']$, where t' denotes the limit of the simulation window, the digitized initial contact geometry $hi(x_1, x_2)$, the contact compliance, i.e. the creep compliance function $\Phi(t)$ for the viscoelastic material.

2. Adopt the initial guess for the computational domain *P*. If during application of additional time increments the current contact area reaches the boundaries of the considered computational domain, the contact simulation has to be restarted with a larger domain.

3. Establish the discretization parameters: $N_1, \Delta_1, N_2, \Delta_2, N_t, \Delta_t$.

4. Digitize all problems inputs. Obtain $W(k), k = 1 \ldots N_t$, $hi(i, j), (i, j) \in P$, $\Phi(k), k = 1 \ldots N_t$.

5. Compute the array of influence coefficients $K(i, j, k), (i, j) \in P, k = 1 \ldots N_t$, as discussed in [15].

6. Solve an initial contact state ($k = 1$), as a purely elastic contact problem, but with the contact compliance $\Phi(1)$, and obtain the initial pressure distribution $p(i, j, 1), (i, j) \in P$ by using the proposed solution of the instantaneous contact state. In this particular case, the surface displacement is simply the convolution between pressure and the influence coefficients, with no memory effect to account for, equation (17):

$$u(i, j, 1) = \sum_{\ell=1}^{N_1} \sum_{m=1}^{N_2} K(i - \ell, j - m, 1) p(\ell, m, 1), \ (i, j) \in P. \tag{17}$$

7. Increase k (i.e. apply a new time increment) and solve the instantaneous contact state to get $p(i, j, k), (i, j) \in P$. This can be achieved as all historical pressures $p(i, j, 1) \ldots p(i, j, k-1), (i, j) \in P$ are known at this point.

8. If the end of the simulation window is reached (i.e. $k = N_t$), stop program execution and export the computed data. Otherwise, go to step 7.

When the simulation of the memory effect is added as an outer loop, the computational complexity of the algorithm for the simulation of the viscoelastic contact process becomes of order $O(N_t^2 N_1 N_2 \log(N_1 N_2))$. Practically, a viscoelastic contact scenario with a 256×256 spatial discretization and 200 time steps can be solved on a 3 GHz quad-core processor in a matter of minutes. Consequently, the newly advanced algorithm is expected to tackle rough contact simulations involving real microtopography data obtained from 3D surface imaging devices.

5. Algorithm validation

The novel numerical program was benchmarked against the partially analytical solution derived by Ting [5,6] for the Maxwell and the Zener viscoelastic half-spaces indented by a rigid spherical punch of radius R in a step loading $W(t) = W_0 H(t)$, where $H(t)$ denotes the Heaviside step function, and W_0 is fixed but otherwise arbitrarily chosen. The Maxwell rheological model consists in a spring of shear modulus G connected in series with a dashpot of viscosity η. The relaxation time for the Maxwell material, namely the time it takes for stress to decay by a factor of e (i.e. the Euler's number), is $\tau = \eta / G$. The creep compliance of the Maxwell viscoelastic half-space can be expressed as $\Phi(t) = 1/(2G)(1 + t/\tau)$. The Ting's model [5,6] yields the following equation for the pressure distribution achieved at time t after the first contact, at the radial coordinate r, equation (18):

$$p(t,r)=\frac{8G}{\pi R}\left(\left(a(t)^2-r^2\right)^{\frac{1}{2}}-\frac{1}{\tau}\int_0^t\exp\left(\frac{t'-t}{\tau}\right)\mathrm{Re}\left(\left(a(t')^2-r^2\right)^{\frac{1}{2}}\right)dt'\right), \tag{18}$$

where $a(t)$ denotes the contact radius at time t, $a(t)=\left(3RW_0\Phi(t)/8\right)^{1/3}$, and Re() the real part of its complex argument.

The Maxwell and Kelvin models are adequate for qualitative or conceptual analyses, but quantitative representation of the behavior of real materials requires an increase in the number of parameters. The Standard Linear Solid Model, also known as the Zener model, can be represented as a spring of shear modulus G in series with a Kelvin model of parameters G_K and η_K, or as a spring in parallel with a Maxwell model. The creep compliance function of the Zener viscoelastic half-space can be expressed as, equation (19):

$$\Phi(t)=\frac{1}{2}\left(\frac{1}{G}+\frac{1}{G_K}\left(1-\exp\left(-\frac{t}{\tau}\right)\right)\right),\ \text{where}\ \tau=\eta_K/G_K\ . \tag{19}$$

The Zener model exhibits instantaneous elastic strain when stress is instantly applied; if the stress is held constant, the strain creeps towards a limit, whereas, under constant strain, the stress relaxes towards a limit. Moreover, when stress is removed, instantaneous elastic recovery occurs, followed by gradual recovery towards vanishing strain. Using Ting's formalism [5, 6], the pressure distribution results as, equation (20):

$$p(t,r)=\frac{8G}{\pi R}\left(\left(a(t)^2-r^2\right)^{\frac{1}{2}}-\frac{1}{\tau}\int_0^t\exp\left(\frac{2(t'-t)}{\tau}\right)\mathrm{Re}\left(\left(a(t')^2-r^2\right)^{\frac{1}{2}}\right)dt'\right), \tag{20}$$

with the contact radius $a(t)=\left(3RW_0\Phi(t)/8\right)^{1/3}$.

The pressure distributions predicted by the newly advanced computer program at several times after the first contact, depicted with continuous red lines in figures 1 and 2, match well the data resulting from numerical computation of relations (18) and (20), respectively, displayed using dashed grey lines. Dimensionless pressure distribution and radial coordinate are defined as ratio to Hertz central pressure p_H and contact radius a_H, both corresponding to the maximum loading level W_0. The good agreement between the two data sets legitimize the novel algorithm for viscoelastic contact simulation.

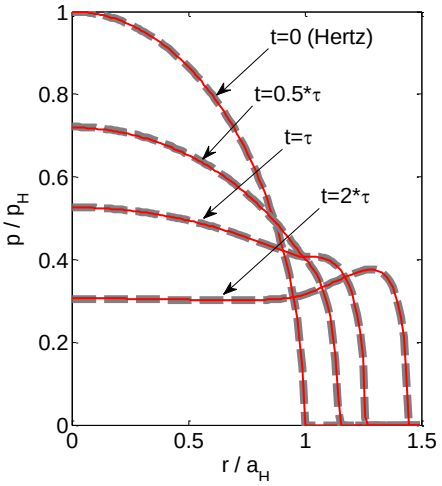

Figure 1. Comparison of pressure history in the step loading spherical indentation of a Maxwell half-space.

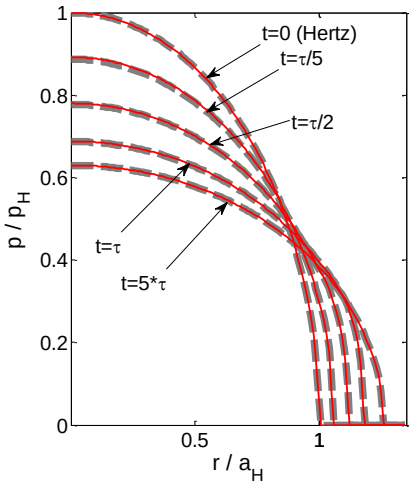

Figure 2. Comparison of pressure history in the step loading spherical indentation of a Zener half-space.

6. Conclusions

A robust algorithm for the simulation of linear viscoelastic contact processes is advanced in this paper, by coupling an updated algorithm for the contact of purely elastic materials with a semi-analytical method for the computation of viscoelastic displacement. Reproduction of the memory effect characteristic to viscoelastic materials is achieved by imposing a temporal discretization, and by assessing the instantaneous contact state at every new time step, based on all previous states. The solution of the set of equations and inequalities describing each instantaneous contact state is obtained in an iterative manner, in which both pressure distribution and contact area are iterated simultaneously.

Compared to other existing methods, the new approach can readily handle arbitrary contact geometry, arbitrary creep compliance information (which can be inputted in discrete form as resulting from experimental data, without the need for additional fitting) and arbitrary loading programs. The updated elastic contact solver is based on the conjugate gradient method, whose convergence is guaranteed. The computational efficiency is increased using a well-established method for rapid calculation of convolution products.

The novel numerical program was benchmarked against partially analytical existing results for linear viscoelastic half-spaces described by Maxwell or Zener rheological models, indented by a spherical punch in step loading. In both cases, a good validation was found, giving confidence in the algorithm ability to solve a large variety of viscoelastic contact scenarios.

Acknowledgement

This work was partially supported from the project “Integrated Center for Research, Development and Innovation in Advanced Materials, Nanotechnologies, and Distributed Systems for Fabrication and Control”, Contract No. 671/09.04.2015, Sectoral Operational Program for Increase of the Economic Competitiveness co-funded from the European Regional Development Fund.

References

[1] Sneddon I N 1965 *Int. J. Engng Sci.* **3** 47
[2] Lee E H and Radok J R M 1960 *ASME J. Appl. Mech.* **27** 438
[3] Hunter S C 1960 *J. Mech. Phys. Solids* **8** 219
[4] Yang W H 1966 *ASME J. Appl. Mech.* **33** 395
[5] Ting T C T 1966 *ASME J. Appl. Mech.* **33** 845
[6] Ting T C T 1968 *ASME J. Appl. Mech.* **35** 248
[7] Greenwood J. A 2010 *Int. J. Mech. Sci.* **52** 829
[8] Renouf M, Massi F, Fillot N and Saulot A 2011 *Tribol. Int.* **44** 834
[9] Kozhevnikov I F, Cesbron J, Duhamel D, Yin H P and Anfosso-Ledee F 2008 *Int. J. Mech. Sci.* **50** 1194
[10] Chen W W, Wang Q J, Huan Z and Luo X 2008 *ASME J. Tribol.* **133** 041404
[11] Kozhevnikov I F, Duhamel D, Yin H P and Feng Z Q 2010 *Int. J. Mech. Sci.* **52** 399
[12] Polonsky I A and Keer L M 1999 *Wear* **231** 206
[13] Spinu S 2014 *J. Balk. Tribol. Assoc.* **20** 63
[14] Spinu S and Glovnea M 2012 *J. Balk. Tribol. Assoc.* **18** 195
[15] S Spinu and D Gradinaru 2015 *IOP Conf. Ser.: Mater. Sci. Eng.* **95** 012111
[16] Liu S B, Wang Q and Liu G 2000 *Wear* **243** 101